Implementation of Tracking and Capturing a Moving Object using a Mobile Robot

Sang-joo Kim, Jin-woo Park, and Jang-Myung Lee

Abstract: A new scheme for a mobile robot to track and capture a moving object using camera images is proposed. The moving object is assumed to be a point-object and is projected onto an image plane to form a geometrical constraint equation that provides the position data of the object based on the kinematics of the active camera. Uncertainties in position estimation caused by the point-object assumption are compensated for using the Kalman filter. To generate the shortest time path to capture the moving object, the linear and angular velocities are estimated and utilized. In this paper, the experimental results of the tracking and capturing of a target object with the mobile robot are presented.

Keywords: Mobile robot, Kalman filter, tracking & capturing, active camera.

1. INTRODUCTION

Mobile robots have many application fields because of their high workability [1-6]. They are especially necessary for tasks that are difficult and dangerous for men to perform [22]. Many researchers have shown interest in mobile robots. Most researchers have focused on successful navigation [18-21], that is, on reaching a fixed target point safely [7,8,10,12]. However, if a mobile robot is working under water or in space, the target object may move freely [11,14,22]. Therefore, the ability of a mobile robot to process moving targets is necessary. If an active camera system is applied to navigation and the tracking of moving objects, there will be many advantages [18,20]. An active camera system capable of panning and tilting should be able to automatically calibrate itself and keep track of an object of interest for a longer time interval without movement of the mobile robot [1]. There are several approaches [13,15-17] that can be used to overcome the uncertainties of measuring the locations of the mobile robot or other objects.

In this paper, the position of an object was estimated using the kinematics of an active camera and images of the object, which was assumed to be flat and small on the floor its linear and angular velocities were estimated for the mobile robot, To predict the future trajectory of the object, which plans the shortest time path on which to track and capture the moving object. For a simple example, in a pick and place operation with a manipulator, the precise motion estimation of an object on a conveyor belt is a critical factor for the successful operation of the stable grasping. A well-structured environment such as a moving-jig that carries object on conveyor belt and stops when the manipulator grasps the object obviates the motion estimation requirement.

However, a well-structured environment limits the flexibility of a production line, requires skillful designers for the jig, and high maintenance expense ; eventually it will disappeared from the automated production lines.

To overcome these problems—to grasp a moving object stably without stopping the motion- trajectory prediction of the moving object on the conveyor belt is necessary. The manipulator control system needs to estimate the most accurate position, velocity, and acceleration at any instance to capture the moving object safely without collision and to lift up the object stably without slippage. When the motion trajectory is not high- random and continuous, it can be model analytically to predict the near- future values based on the measured previously data.

A state estimator was designed to overcome the uncertainties in the image data caused by the point-object assumption and physical noises, using a Kalman filter. Based on the estimated velocities of the object, the attitude of the active camera was controlled to locate images of the object on the center of the image frame.

In Section 2, we discuss how to establish a model

Manuscript received February 6, 2003; revised January 5, 2005; accepted June 17, 2005. Recommended by Editorial Board member In So Kweon under the direction of Editor Keum-Shik Hong.

Sang-joo Kim and Jang-Myung Lee are with the School of Electrical Engineering, Pusan National University, San 30 Jangjeon-Dong, Kumjung-ku, Pusan 609-375, Korea. (e-mails: ksj_elec@hanmail.net, jmlee@pusan.ac.kr).

Jin-woo Park is with the Institute of Information Technology Assessment (IITA) 52, Eoeun-dong, Yuseong-gu, Daejeon 305-806, Korea (e-mail: jinu@iita.re.kr).

of an active camera. Section 3 deals with the problem of trajectory estimation of a moving object, and Section 4 deals with the motion planning involved in capturing a moving object. In Section 5, the advantages of our proposed method are illustrated through a simulation and experimental results. Section 6 presents conclusions drawn from this work.

2. ACTIVE CAMERA SYSTEM

In this section, some equations regarding image processing are derived considering the kinematics of the actuators of the active camera.

2.1. Kinematics of the actuators of the active camera system

The active camera system has the ability to pan and tilt, as shown in Fig. 1. The position and posture of the camera are defined with respect to the base frame. According to the Denavit - Hartenberg convention, a homogeneous matrix can be obtained after establishing the coordinate system and representing parameters, as shown in Table 1 and (1).

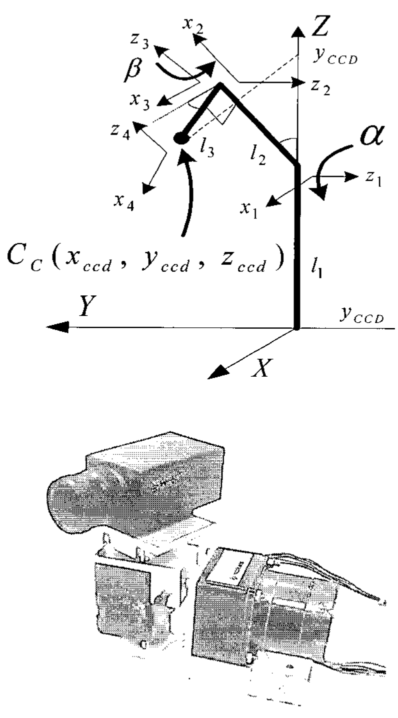

Fig. 1. 2-D.O.F Camera platform (Left) and its real image (Right).

Table 1. DH link parameters.

Link	θ	D	a	α
1	0	l_1	0	-90°
2	90°- α	0	l_2	0
3	90°	0	0	90°
4	β	0	l_3	0

$$ {}^0H_4 = {}^0H_1 \cdot {}^1H_2 \cdot {}^2H_3 \cdot {}^3H_4 = \tag{1}$$
$$\begin{bmatrix} \cos(\alpha)\cos(\beta) & -\cos(\alpha)\sin(\beta) & \sin(\alpha) & l_2\sin(\alpha)+l_3\cos(\alpha)\cos(\beta) \\ \sin(\beta) & \cos(\beta) & 0 & l_S\sin(\beta) \\ -\sin(\alpha)\cos(\beta) & \sin(\alpha)\cos(\beta) & \cos(\alpha) & l_1+l_2\cos(\alpha)-l_3\sin(\alpha)\cos(\beta) \\ 0 & 0 & 0 & 1 \end{bmatrix}$$

In Fig. 1, Cc (x_{ccd}, y_{ccd}, z_{ccd}) represents a position vector from the center of the mobile robot to the center of the camera lens. Each component of the vector can be represented with respect to the tilting angle, α, and the panning angle, β, of the CCD camera, as follows:

$$x_{ccd} = l_2\sin(\alpha) + l_3\cos(\alpha)\cos(\beta), \tag{2}$$
$$y_{ccd} = l_3\sin(\beta), \tag{3}$$
$$z_{ccd} = l_1 + l_2\cos(\alpha) - l_3\sin(\alpha)\cos(\beta). \tag{4}$$

Also, the attitude vector of the homogeneous matrix represents Roll(θ_R), Pitch(θ_P) and Yaw(θ_Y) angles by tilting and panning angles of the camera as follows:

$$\theta_R = \tan^{-1}\left(\frac{\sin(\alpha)\sin(\beta)}{\sqrt{\cos^2(\alpha)\sin^2(\beta)+\cos^2(\beta)}}\right), \tag{5}$$
$$\theta_P = \tan^{-1}\left(\frac{\sin(\alpha)\cos(\beta)}{\sqrt{\cos^2(\alpha)\cos^2(\beta)+\sin^2(\beta)}}\right), \tag{6}$$
$$\theta_Y = \beta. \tag{7}$$

2.2. Relation between a camera and real coordinates

To measure the distance from a camera to an object using the camera images, at least two image frames that are captured for the same object at different locations are necessary. Usually, a stereo-camera system is used to obtain distance information [24]. However, because there exist uncertainties in feature point matching, this process requires too much time to be implemented in real-time.

The new approach presented in this paper requires only a frame to measure the distance to the object from the CCD camera. Since this approach becomes possible by assuming that a point-object is located on the floor, there also exist uncertainties in position estimation.

To both minimize the uncertainty in position estimation and to estimate the velocities of the moving object, a state estimator was based on the Kalman filter designed.

To render make a real- time tracking and capturing system, the distances in 3D space are calculated using an image frame, based on the assumption that objects are located on a flat floor. Note that since a mobile robot with a parallel-jaw gripper grasps an object on the floor, the height of the object is not an important factor. The image coordinates for the point object, (j, k), are transformed into image center coordinates that are orientation invariant relative to the Roll angle in (6), θ_R, and the size of the image frame, P_x and P_y, (j', k')

$$\begin{bmatrix} j' \\ k' \end{bmatrix} = \begin{bmatrix} \cos(\theta_R) & -\sin(\theta_R) \\ \sin(\theta_R) & \cos(\theta_R) \end{bmatrix} \begin{bmatrix} j - \frac{P_x}{2} \\ k - \frac{P_y}{2} \end{bmatrix}, \tag{8}$$

where P_x and P_y represent the x- and y- directional size of the image frame in pixels, respectively.

To estimate the real location, (x_0, y_0), $\hat{\theta}_0$ and $\hat{r}_0$ are estimated using the linear relationship between the real object range within the view angle and the image frame. That is, for a given set of ($\hat{\theta}_0$, $\hat{r}_0$), there is one-to-one correspondence between the real object point and the image point.

When an point image is captured at (j', k') on the image center frame, the real object position, $\hat{\theta}_0$ and

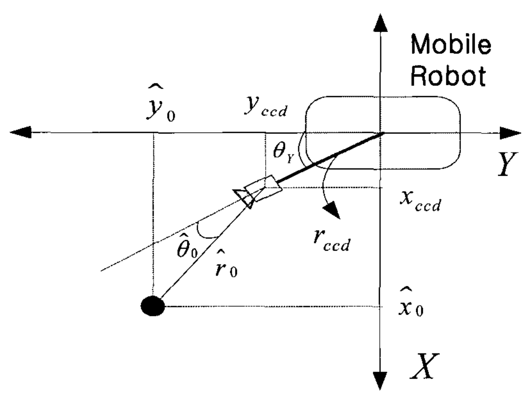

Fig. 2. Estimation of position information from a mobile robot.

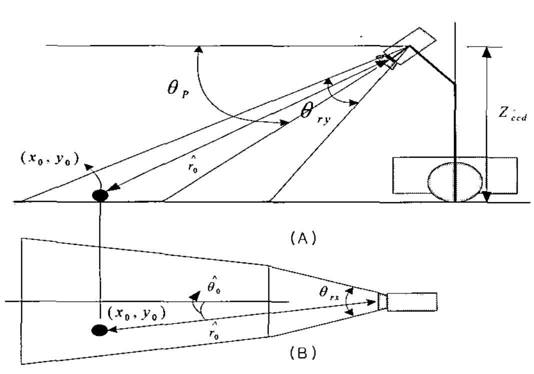

Fig. 3. Estimation of $\hat{r}_0$ (A) and $\hat{\theta}_0$ (B).

$\hat{r}_0$ can be estimated as follows, and as it is illustrated in Fig. 3:

$$\hat{r}_0 = \frac{z_{ccd}}{\cos(\frac{\pi}{2} - \theta_P + \frac{k'}{P_y}\theta_{ry})}, \tag{9a}$$

$$\hat{\theta}_0 = \frac{j'}{P_x}\theta_{rx}, \tag{9b}$$

where θ_{rx} and θ_{ry} represent the x- and y- directional view angles of the CCD camera, respectively. The position of the object with respect to the robot coordinates, (x, y), can be estimated using $\hat{\theta}_0$ and $\hat{r}_0$ [8] as follows:

$$\hat{x}_0 = r_{ccd} \cdot \cos(\theta_Y) + \hat{r}_0 \cdot \cos(\theta_Y + \hat{\theta}_0), \tag{10}$$

$$\hat{y}_0 = r_{ccd} \cdot \sin(\theta_Y) + \hat{r}_0 \cdot \sin(\theta_Y + \hat{\theta}_0), \tag{11}$$

where θ_Y represents the angle between the robot and the active camera, and $r_{ccd}(=\sqrt{x_{ccd} + y_{ccd}})$ represents the distance from the robot to the center of the camera.

2.3. Inverse kinematics to place the center of an image at the desired position

In the case of using an active camera, visual information on the area to be searched can be obtained through the inverse kinematics. The inverse kinematics equations that describe the attitude of the actuator and are used to place the center of an image at a desired position, can be derived from (2)-(4) as follows:

$$\alpha_d = \cos^{-1}\left(\frac{-l_1 l_2 + \sqrt{l_1^2 l_2^2 - (l_1^2 + r_d^2)(l_1^2 - r_d^2)}}{(l_1^2 + r_d^2)}\right)\left(\frac{1}{\sin(\beta_d)}\right), \tag{12}$$

$$\beta_d = \tan^{-1}\left(\frac{y_d}{x_d}\right), \tag{13}$$

where α_d and β_d are the attitude of the camera, (x_d,y_d) represents the desired position of the camera, and r_d is $\sqrt{x_d^2 + y_d^2}$. Table 2 shows the parameters for the camera system, that were used in (12) and (13).

Table 2. Parameters for the active camera system.

l_1	40 cm	l_2	7.5 cm
l_3	4 cm		
P_x	320pixel	P_y	240 pixel
θ_{rx}	50°	θ_{ry}	40°

3. ACTIVE CAMERA SYSTEM

3.1. Modeling of a moving object

When the velocity and acceleration of the target object can be estimated, the next target position $(\hat{T}_x, \hat{T}_y)$ can be predicted as follows [2]:

$$\hat{T}_{x+\delta t} = \hat{T}_x + \hat{V}_x \delta t + \frac{1}{2}\hat{A}_x \delta t^2, \tag{14}$$

$$\hat{T}_{y+\delta t} = \hat{T}_y + \hat{V}_y \delta t + \frac{1}{2}\hat{A}_y \delta t^2, \tag{15}$$

where δt is the sampling time, and $(\hat{T}_x, \hat{T}_y)$, $(\hat{V}_x, \hat{V}_y)$ and $(\hat{A}_x, \hat{A}_y)$ are the current Cartesian coordinate estimates of the target position, velocity and acceleration respectively.

The movement of the object can be decomposed into the linear velocity element and the angular velocity element, ; X-Y coordinates, as follows [3]:

$$\begin{aligned}\delta x_{k+\delta t,k} &= v_k \delta t \cos(\theta_k + \frac{1}{2}\omega_k \delta t) \\ &\approx v_k \cos(\theta_k)\delta t - \frac{1}{2}\omega_k v_k \sin(\theta_k)\delta t^2,\end{aligned} \tag{16}$$

$$\begin{aligned}\delta y_{k+\delta t,k} &= v_k \delta t \sin(\theta_k + \frac{1}{2}\omega_k \delta t) \\ &\approx v_k \sin(\theta_k)\delta t + \frac{1}{2}\omega_k v_k \cos(\theta_k)\delta t^2,\end{aligned} \tag{17}$$

$$\delta\theta_{k+\delta t,k} = \omega_k \delta t, \tag{18}$$

$$\delta v_{k+\delta t,k} = \xi_v, \tag{19}$$

$$\delta\omega_{k+\delta t,k} = \xi_\omega, \tag{20}$$

where v_k and w_k are the linear velocity and angular velocity of the target object, and ξ_v and ξ_ϖ are the variations of linear velocity and angular velocity, respectively. From (16)-(20), we can obtain the state transition matrix, as follows:

$$\begin{aligned}\mathbf{x}_k &= \Phi_{k,k-1}\mathbf{x}_{k-1} + \mathbf{w}_{k-1}, \\ \mathbf{Z}_k &= \mathbf{H}_k \mathbf{x}_k + \mathbf{v}_k,\end{aligned} \tag{21}$$

where $\mathbf{x}_k = \begin{bmatrix} x_k & y_k & \theta_k & v_k & \omega_k \end{bmatrix}$,

$$\Phi_{k,k-1} = \begin{bmatrix} 1 & 0 & 0 & \delta t\cos(\theta_{k-1}) & -\frac{1}{2}v_{k-1}\delta t^2 \sin(\theta_{k-1}) \\ 0 & 1 & 0 & \delta t\sin(\theta_{k-1}) & \frac{1}{2}v_{k-1}\delta t^2 \cos(\theta_{k-1}) \\ 0 & 0 & 1 & 0 & \delta t \\ 0 & 0 & 0 & 1 & 0 \\ 0 & 0 & 0 & 0 & 1 \end{bmatrix},$$

$$\mathbf{w}_{k-1} = \begin{bmatrix} 0 \\ 0 \\ 0 \\ \xi_v \\ \xi_\omega \end{bmatrix}, \mathbf{Z}_k = \begin{bmatrix} x_k \\ y_k \end{bmatrix}, \mathbf{H}_k = \begin{bmatrix} 1 & 0 & 0 & 0 & 0 \\ 0 & 1 & 0 & 0 & 0 \end{bmatrix},$$

and $\mathbf{v}_k = \begin{bmatrix} \gamma_x \\ \gamma_y \end{bmatrix}$.

Notice that Φ_k is the state transition matrix, $\mathbf{w}_k$ is the vector representing process noise, $\mathbf{Z}_k$ is the measurement vector, $\mathbf{H}_k$ represents the relationship between the measurement and the state vector, and γ_x and γ_y are x- and y- directional measurement errors, respectively.

3.2. State estimation of a moving object based on a Kalman filter

Input data such as image information include uncertainties and noises generated during the data capturing and processing steps. The state transition of a moving object also includes irregular components. Therefore, as a robust state estimator against these irregularities, a Kalman filter was adopted to form a state observer [11-14]. The Kalman filter minimizes the estimation error by modifying the state transition model, based on the error between the estimated vectors and the measured vectors, with an appropriate filer gain. The state vector, which consists of the position on the x-y plane, linear/angular velocities, and linear/angular accelerations, can be estimated using the measured vectors representing the position of a moving object on the image plane.

The covariance matrix of estimated error must be calculated to determine the filter gain. The projected estimate of the covariance matrix of estimated error is represented as

$$P_k' = \Phi_{k,k-1}P_{k-1}\Phi_{k,k-1}^T + Q_{k-1}, \tag{22}$$

where P_k' is a zero-mean covariance matrix representing the prediction error, Φ_k represents the system noise, P_{k-1} is the error covariance matrix for the previous step, and Q_{k-1} represents other measurement and computational errors . The optimal filter gain K_k that minimizes the errors associated with the updated estimate is

$$K_k = P_k' H_k^T [H_k P_k' H_k^T + R_k]^{-1}, \tag{23}$$

where H_k is the observation matrix and R_k is the zero-mean covariance matrix of the measurement noise.

The estimate of the state vector $\hat{x}_k$ from the measurement Z_k is expressed as

$$\hat{x}_k = \Phi_{k,k-1}\hat{x}_{k-1} + K_k[Z_k - H_k\Phi_{k,k-1}\hat{x}_{k-1}]. \quad (24)$$

Therefore, $\hat{x}_k$ is updated based on the new values provided by Z_k. The error covariance matrix that will be used for the prediction, P_k, can be updated as follows [4,9]:

$$P_k = P_k' - K_k H_k P_k'. \quad (25)$$

After the current time is updated to $k+1$, a new estimation can be provided using (23) to (26).

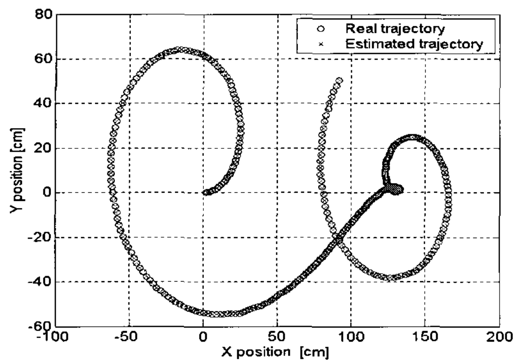

(a) Trajectory of moving object.

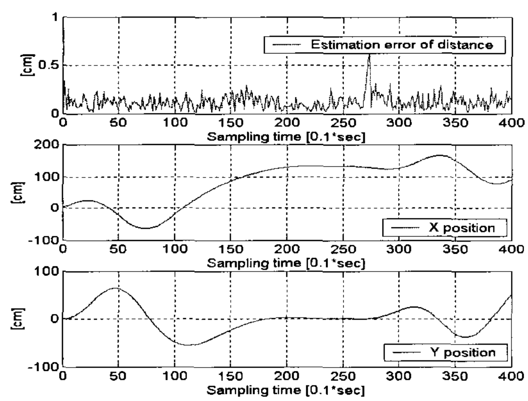

(b) Estimation |error| along the trajectory.

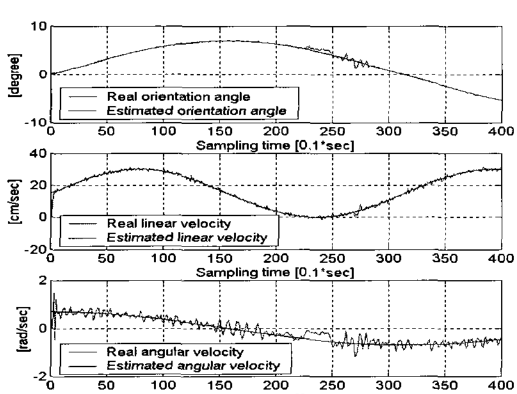

(c) State estimations, θ_k, v_k, and ω_k, using a Kalman filter.

Fig. 4. State estimations using a Kalman filter.

Fig. 4(a) represents the real and an estimated trajectories of a moving object, and Fig. 4(b) represents the estimation |error| when the trajectory was estimated using the Kalman filter. To incorporate the measurement noise, which is empirically assumed to be zero-mean, Gaussian random noise with a variance of 2, the linear and angular velocities of the object were set as follows:

$$\begin{aligned} v_k &= 15*(\sin(0.02*k)+1) + \xi_v \quad [\text{ cm/sec}], \\ \omega_k &= 0.7*\cos(0.01*k) + \xi_\omega \quad [\text{ rad/sec}], \end{aligned} \quad (26)$$

where the linear and angular velocities (ξ_v, ξ_w) were assumed to include the Gaussian random noise with the variance of 3 and 0.1, respectively.

Fig. 4 shows that the Kalman filter estimation of the states under a noisy environment.

3.3. Trajectory estimation of a moving object

The states of a moving object can be estimated if the initial state and input are given for the state transition model. Therefore, the states can be estimated for the next inputs by estimating the linear velocity and angular velocity of the moving object using the Kalman filter as a state estimator.

From the linear velocity/acceleration and rotational angular velocity/acceleration data, the next states can be approximated, as in the following first order equations:

$$v_{k+n} = \hat{v}_k + \hat{a}_{lk} nT, \quad (27)$$

$$\omega_{k+n} = \hat{\omega}_k + \hat{a}_{\omega k} nT. \quad (28)$$

In Fig. 4(c), the result the noise includes possible noise since it is a dynamically varying system, although is surpressed by the Kalman filter. Therefore, the least square estimation method is utilized, which has robust anti-noise characteristics [23].

From the estimated inputs and using the state transition model, the trajectory of a moving object can be estimated as follows:

$$\hat{x}_{k+m} = x_k + \sum_{h=0}^{m} v(h)\cos[\theta(h)]T, \quad (29a)$$

$$\hat{y}_{k+m} = y_k + \sum_{h=0}^{m} v(h)\sin[\theta(h)]T, \quad (29b)$$

$$v(h) = \hat{v}_k + \hat{a}_{lk} hT, \quad (29c)$$

$$\theta(h) = \hat{\theta}_k + \hat{\omega}_k hT + \frac{1}{2}\hat{a}_{\omega k} hT^2. \quad (29d)$$

4. MOTION PLANNING FOR CAPTURING

To capture a moving object, the mobile robot needs to be controlled while considering the relation between the position of the mobile robot and the position of the moving object. Fig. 5 shows the motion planning process of a mobile robot for the process of capturing a moving object.

The mobile robot estimates the position of the moving object within m sampling time and selects the shortest distance from its current position to the moving object, assuming that its location is known *a priori*. The localization scheme of the mobile robot using the information on the moving object, which improves the accuracy in capturing, was developed in [14]. The target point of the mobile robot at the k-sampling time is denoted as $\hat{x}_R(k+m)$, which is one of the estimated points of the mobile robot after m sampling time.

$$\hat{x}_R(k+m_{opt}) = \min_{m=1\sim M} \left\| \hat{x}_O(k+m) - \hat{x}_R(k+m) \right\|, \quad (30)$$

where $\hat{x}_R(k+m)$ is the position of the mobile robot after m sampling time, and given that the mobile robot moves along the shortest path towards the target point $\hat{x}_O(k+m)$.

The position of the moving object in the Cartesian coordinate system is acquired using the relation between image frames. The linear and angular velocities of the moving objects are estimated by the state estimator. The Kalman filter is used as a state estimator to determine the characteristics of the robustness of noises and uncertainties included in the input data.

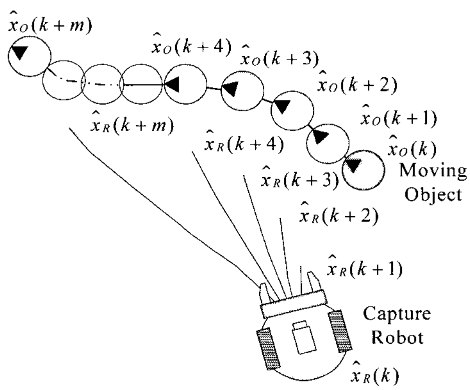

Fig. 5. Estimation of the trajectory for capturing.

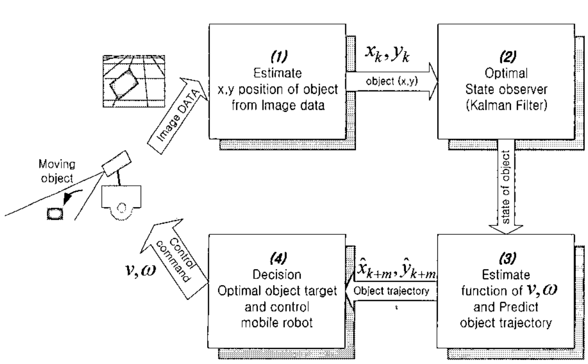

Fig. 6. Mobile robot control for tracking.

After estimating the trajectory of the target object, the optimal trajectory and motion planning of the mobile robot are determined in order to capture the target object in the shortest time. Fig. 6 shows the overall structure of mobile robot control to capture a target object.

5. SIMULATIONS AND EXPERIMENTS

To demonstrate and illustrate the proposed method, we present an example. It is assumed that the velocity limit of a mobile robot is 30 cm/sec and that the camera is installed on top of the mobile robot. The initial locations of the mobile robot and the moving object are (-50, -50 cm) and (-250, 300 cm) in with respect to the reference frame, respectively. The velocity and angular velocity of the moving object are as follows:

$$v_k = 30(\cos(0.01k)+1) + \xi_v \quad [cm/\sec], \quad (31a)$$

$$\omega_k = 0.7\sin(0.03k + \frac{\pi}{1.5}) + \xi_\omega \quad [rad/\sec]. \quad (31b)$$

The forward direction and rotational angular velocity of the moving object are Gaussian random variables with variances of 2 and 0.1, respectively, which are obtained experimentally. Fig. 7(a) illustrates the trajectory of a moving object and shows the mobile robot trying to capture the object by estimating its trajectory. Fig. 7(b) shows the distance between the mobile robot and the moving object, the error between

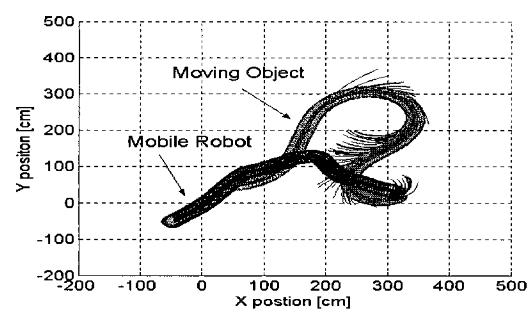

(a) Trajectory.

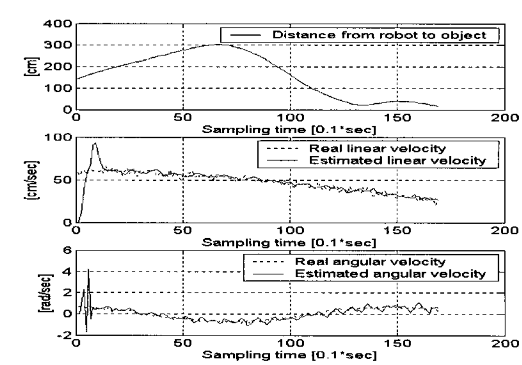

(b) Estimated state.

Fig. 7. Results of simulation.

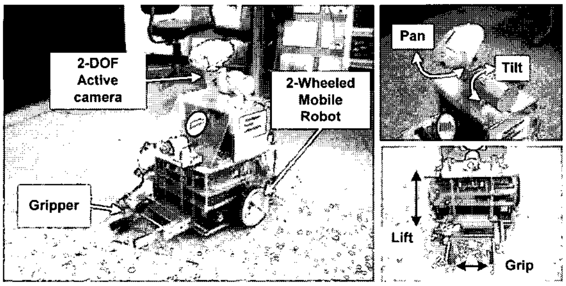

Fig. 8. Components of ZIRO.

the estimated velocity and the real velocity, and the error between the estimated angular velocity and the real angular velocity. Although the errors of the estimated velocities are high at first, they converge to zero immediately.

Experiments that included the proposed algorithm were applied to a mobile robot named ZIRO that was developed in the Intelligent Robot Laboratory, PNU [5], as shown in Fig. 8.

ZIRO, recognizes an object in the 3D space, approaches the object to capture it, and carries it to a goal position. For this purpose, ZIRO has a 2 d.o.f active camera to search and to track an object and a gripper to capture the object. The two-wheel differential driving mechanism supports flexible motion on a floor following the commands based on the image captured by the 2 d.o.f pan/tilt camera. To control the wheels in real time, a distributed control system using a CAN-based network was implemented. Three CAN-based controllers are connected to the network, among which the main controller gathers the gyro sensor data and sends them to the wheel controllers. The CAN network is connected to a higher-level ISA bus that connects the 2 d.o.f pan/tilt camera controllers to the main controller (a Pentium PC board). Every 100 msec, the position of an object in 3D space was calculated using the posture of the camera and the object position on the image frame to plan the trajectory of the mobile robot. The planned trajectory commands were sent to the wheel controllers that use a PID algorithm to control the angle every 10 msec. The functional structure of the mobile robot is illustrated in Fig. 9.

Two experiments were performed to show the tracking and capturing of a mobile object. Fig. 10 shows the experimental results of tracking a moving object, an 8x6[cm] red-colored mouse of two wheels with random velocities in the range of 25-35[cm/sec]. First, ZIRO detected the moving object using an active camera. When the moving object was within view, ZIRO tracked it according to following the proposed method.

Fig. 11 illustrates that the mobile robot captured a ball, moved to the target point and put the ball on the target point. The minimum path was estimated using the trajectories of the mobile robot and the object, while

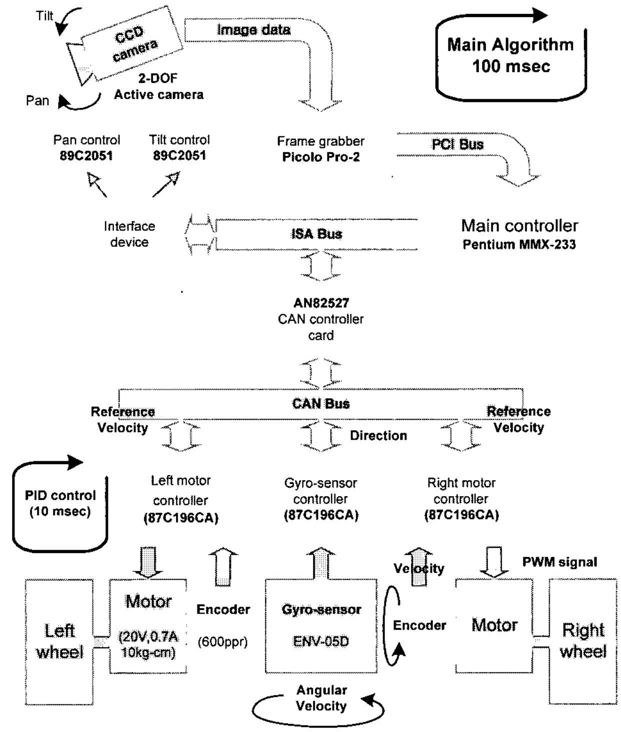

Fig. 9. Functional structure of the mobile robot.

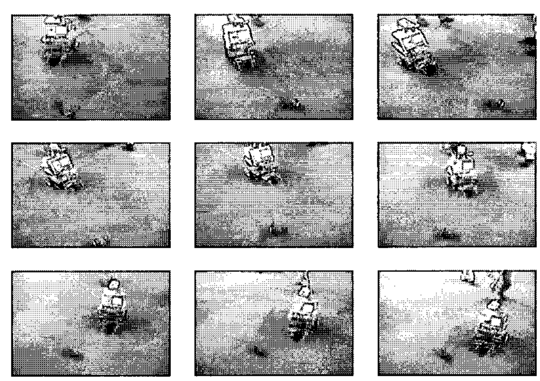

Fig. 10. The results for tracking a moving object.

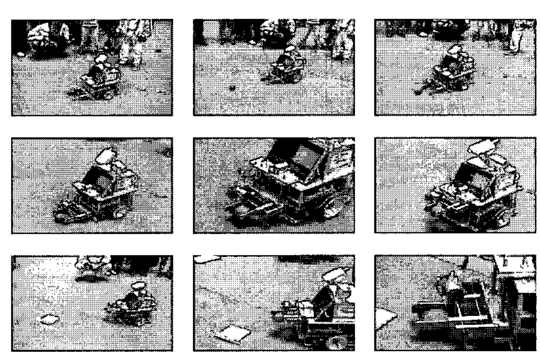

Fig. 11. Experimental results for capturing a ball.

the robot was tracking the object. Object the object was grasped firmly with the aid of the touch sensors is in the gripper.

6. CONCLUSION

This paper proposes a method of tracking and capturing a moving object using an active camera mounted on a mobile robot. The effectiveness of the proposed method was demonstrated by simulations and experiments, and was verified through the following procedure.

1. Position estimation of a target object based on the kinematic relationship of consecutive image frames.
2. Movement estimation of the target object using a Kalman filter for tracking.
3. Motion planning of a mobile robot to capture the target object within the shortest time, based on its estimated trajectory.

This method approach enables real- time tracking and capturing operations since it extracts the distance information from a single image frame and estimates the next motion using the Kalman filter that provides a closed- form solution.

REFERENCES

[1] K. Daniilidis and C. Krauss, "Real-time tracking of moving objects with an active camera," *Real-Time Imaging*, Academic Press Limited, 1998.

[2] R. F. Berg, "Estimation and prediction for maneuvering target trajectories," *IEEE Trans. on Automatic Control*, vol. AC-28, no. 3, pp. 294-304, March 1983.

[3] S. M. Lavalle and R. Sharma, "On motion planning in changing partially predictable environments," *International Journal of Robotics Research*, vol. 16, no. 6, pp. 705-805, December 1997.

[4] H. W. Sorenson, "Kalman filtering techniques," *Advances in Control Systems Theory and Applications*, vol. 3, pp. 219-292, 1996.

[5] J. W. Park and J. M. Lee, "Robust map building and navigation for a mobile robot using active camera," *Proc. of ICMT*, pp. 99-104, October 1999.

[6] R. A. Brooks, "A robust layered control system for a mobile robot," *IEEE Journal of Robotics and Automation*, vol. RA-2, no. 1, pp. 14-23, April 1986.

[7] J. J. Leonard and H. F. Durrant-Whyte, "Mobile robot localization by tracking geometric beacons," *IEEE Trans. on Robotics and Automation*, vol. 7, no. 3, pp. 376-382, June 1991.

[8] D. J. Kriegman, E. Triendl, and T. O. Binford, "Stereo vision and navigation in buildings for mobile robots," *IEEE Trans. on Robotics and Automation*, vol. 5, no. 6, pp. 792-803, December 1989.

[9] R. E. Kalman, "A new approach to linear filtering and prediction problems," *Trans, ASME, J. Basic Eng*, vol. 82D, pp. 35-45, March 1960.

[10] M. Y. Han, B. K. Kim, K. H. Kim, and J. M. Lee, "Active calibration of the robot/camera pose using the circular objects," *Trans. on Control, Automation and Systems Engineering*, vol. 5, no. 3, pp. 314-323, April 1999.

[11] D. Nair and J. K. Aggarwal, "Moving obstacle detection from a navigation robot," *IEEE Trans. on Robotics and Automation*, vol. 14, no. 3, pp. 404-416, 1989.

[12] A. Lallet and S. Lacroix, "Toward real-time 2D localization in outdoor environments," *Proc. of the IEEE International Conference on Robotics & Automation*, pp. 2827-2832, May 1998.

[13] A. Adam, E. Rivlin, and I. Shimshoni, "Computing the sensory uncertainty field of a vision-based localization sensor," *Proc. of the IEEE International Conference on Robotics & Automation*, pp. 2993-2999, April 2000.

[14] B. H. Kim, D. K. Roh, J. M. Lee, M. H. Lee, K. Son, M. C. Lee, J. W. Choi, and S. H. Han, "Localization of a mobile robot using images of a moving target," *Proc. of the IEEE International Conference on Robotics & Automation*, May 2001.

[15] V. Caglioti, "An entropic criterion for minimum uncertainty sensing in recognition and localization part II-A case study on directional distance measurements," *IEEE Trans. on Systems, Man, and Cybernetics*, vol. 31, no. 2, pp. 197-214, April 2001.

[16] C. F. Olson, "Probabilistic self-localization for mobile robots," *IEEE Trans. on Robotics and Automation*, vol. 16, no. 1, pp. 55-66, February 2000.

[17] H. Zhou and S. Sakane, "Sensor planning for mobile robot localization based on probabilistic inference using bayesian network," *Proc. of the 4th IEEE International Symposium on Assembly and Task Planning*, pp. 7-12, May 2001.

[18] M. Selsis, C. Vieren, and F. Cabestaing, "Automatic tracking and 3D localization of moving objects by active contour models," *Proc. of the IEEE International Symposium on Intelligent Vehicles*, pp. 96-100, 1995.

[19] H. Choset and K. Nagatani, "Topological simultaneous localization and mapping (SLAM): Toward exact localization without explicit localization," *IEEE Trans. on Robotics and Automation*, vol. 17, no. 2, pp. 125-137, April 2001.

[20] S. Segvic and S. Ribaric, "Determining the absolute orientation in a corridor using projective geometry and active vision," *IEEE Trans. on Industrial Electronics*, vol. 48, no. 3, pp. 696-710, June 2001.

[21] N. Strobel, S. Spors, and R. Rabenstein, "Joint

audio-video object localization and tracking," *IEEE Signal Processing Magazine*, vol. 18, no. 1, pp. 22-31, January 2001.
[22] R. G. Hutchins and J. P. C. Roque, "Filtering and control of an autonomous underwater vehicle for both target intercept and docking," *Proc. of the 4th IEEE International Conference on Control Applications*, pp. 1162-1163, 1995.
[23] J. Jang, C. Sun, and E. Mizutani, *Neuro-Fuzzy and Soft Computing*, Prentice-Hall, 1997.
[24] E. Grosso and M. Tistarelli, "Active/dynamic stereo vision," *IEEE Trans. on Pattern Analysis and Machine Intelligence*, vol. 17, no. 9, pp. 868-879, December 1995.

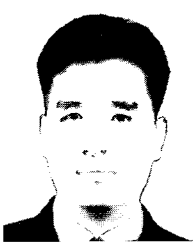

Sang-joo Kim received the Ph.D. degree in Electrical Engineering from Pusan University in 2005. His research interests include robot vision, navigation, and image processing.

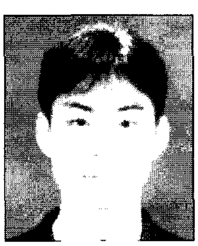

Jin-woo Park received the B.S. degree in Electrical Engineering from Pusan University in 2003. His research interests include nonlinear control, adaptive control, and system identifycation.

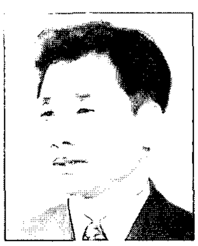

Jang-Myung Lee has been a Professor in the Department of Electronics Engineering at Pusan National University. He received the B.S. and M.S degree in Electrical Engineering from Seoul National University in 1980 and 1982, respectively and the Ph.D. degree in Computer Engineering from the University of Southern California in 1990. His current research interests include intelligent robotic systems, integrated manufacturing systems, cooperative control and sensor fusion. Dr. Lee is an IEEE Senior member and a member of ICASE and IEEK.